

## UV-Vis Absorption Study of *cis*- and *trans*-Poly(phenylacetylene)s Based on CNDO/S Calculation

Fumiaki ISHII<sup>\*,†</sup> Shigeyuki MATSUNAMI,<sup>††</sup> Minako SHIBATA,<sup>††</sup>  
and Toyoji KAKUCHI

<sup>\*</sup> Division of Applied Physics, Graduate School of Engineering, Hokkaido University,  
Sapporo 060-8628, Japan

Division of Bioscience, Graduate School of Environmental Earth Science, Hokkaido University,  
Sapporo 060-8628, Japan

(Received August 12, 1998)

**ABSTRACT:** Before and after the thermal isomerization, the observed ultraviolet-visible (UV-Vis) absorptions of the phenyl groups and conjugated main chain for *cis*- and *trans*-poly(phenylacetylene)s (PPAs) in solution were investigated on the basis of CNDO/S calculation for the *cis*-transoidal and  $\pm\tau^\circ$ -deflected *trans*-transoidal structures. The two kinds of the UV-Vis absorption peaks were observed at 263 and 390 nm for the *cis*-transoidal PPA and at 227 and 248 nm for  $90^\circ$ -deflected *trans*-transoidal PPA, which were due to the  $\pi$ - $\pi^*$  transitions of phenyl groups and the conjugated bonds in the main chain. After *cis*-*trans* isomerization, the larger blue shift of the  $\pi$ - $\pi^*$  transition absorption in the UV spectrum was confirmed from the CNDO/S calculation for the  $\pm 90^\circ$ -deflected *trans*-transoidal structures.

**KEY WORDS** UV-Vis Absorption / *cis*- and *trans*-Poly(phenylacetylene)s / CNDO/S Calculation /

Recently, substituted poly(phenylacetylene) (PPA) have been paid attention as polymeric materials possessing magnetic and nonlinear optical properties.<sup>1</sup> The properties and behaviors of the nonlinear magnetic susceptibilities are characterized by the underlying  $\pi$ -electron and its excitation process in the conjugated bonds, which depend on the molecular chain structures of *cis*-transoidal, *trans*-cisoidal, and *trans*-transoidal forms. However, the thermal isomerization and the chain structures of PPA were not verified largely up to date, because the IR and high resolution NMR spectra after thermal isomerization were complex and broad.<sup>2-4</sup>

In a series of NMR studies,<sup>5,9</sup> we have clarified first that chain structures of PPA in the solid state are *cis*-transoidal and  $\pm 80^\circ$  deflected *trans*-transoidal before and after DSC exotherm at about  $180^\circ\text{C}$ , respectively, and then the exothermic reaction is the *cis*-*trans* isomerization. Especially, it is worth noting that the  $^{13}\text{C}$  peak of main chain carbons in the  $^{13}\text{C}$  NMR spectrum in the solid state for each polymer shifted to upfield by 2–3 ppm after *cis*-*trans* isomerization, in contrast to its downfield shift for polyacetylene.<sup>9</sup> This upfield shift was attributed to the greater electron density on the main chain carbons in the  $\tau = 80^\circ$  deflected angle *trans*-transoidal chain.

It is well-known that the UV-Vis absorption of conjugated polyene as poly(acetylene) (PA) is very dependent on the stereochemical configuration and the effective conjugated length of the main chain. The UV absorption band of the  $\pi$ - $\pi^*$  transition for the *trans*-transoidal configuration are located in a higher wavelength region than that for the *cis*-transoidal one. The wavelength  $\lambda$  of absorption becomes greater as the length of the planar conjugated chain increases and the intensity also increases. In the UV-Vis spectra of PPA solutions, two kinds of the  $\pi$ - $\pi^*$  absorption peaks due

to the conjugated double bonds of main chain and phenyl group have been observed in the wavelength region between 100 and 1000 nm, as well as polyenes. However, after *cis*-*trans* isomerization, the corresponding UV-Vis absorption peaks for annealed PPA sample and their theoretical analyses have apparently not been reported to date.

In this paper, the assignment of observed UV-Vis absorption peaks and the wavelength  $\lambda$  shift of absorption after *cis*-*trans* isomerization for PPA are investigated on the basis of UV theory within semiempirical molecular orbital CNDO/S calculation.<sup>10</sup> The localization of the  $\pi$ -electrons in the conjugated main chain and its UV blue shift due to the deflected *trans*-transoidal form will be discussed.

### EXPERIMENTAL

#### Sample

*cis*- and *trans*-Samples of PPA were prepared by the same method described in previous papers.<sup>5,7,11</sup> Number-average molecular weight and molecular weight distribution were 25000 and 1.76, respectively, for *cis*-PPA and those were 2500 and 1.33, respectively, for *trans*-PPA.

#### UV-Vis Measurements

The UV-Vis spectra of PPA were run on a Hitachi U-3200 spectrophotometer with 10 mm glass cell in  $\text{CHCl}_3$  at room temperature.

#### UV-Vis Absorption Band Calculations

UV-Vis absorption bands of five conformers for PPA were theoretically calculated using CNDO/S<sup>10</sup> with MOS-F of Anchor II software (Fujitsu) on a Fujitsu S-4/5 workstation. The same chain structures of the five

<sup>†</sup> To whom all correspondence should be addressed (Tel: +81+11-706-6642, Fax: +81+11-716-6175, E-mail: fishii@eng.hokudai.ac.jp).

<sup>††</sup> Research Fellowship of the Japan Society for the Promotion of Science.

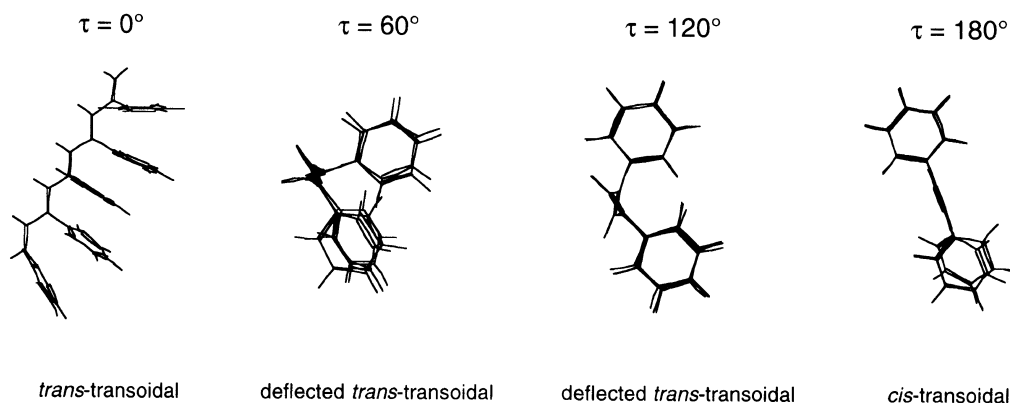


**Figure 1.** The back-bone geometry of the deflected *trans* chain for five conformer of PPA projected on the perpendicular plane to its axis. The deflected angle of  $\tau$  corresponds to the dihedral angle between two double bonds in the main chain.

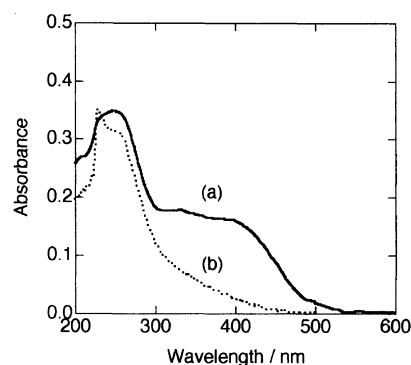
conformers as *cis*- and *trans*-forms determined by AM1 in previous papers were used in the UV transition band, which were *trans*-transoidal, *trans*-cisoidal, *cis*-transoidal, and deflected *trans*-transoidal forms. Although the formation energy of the 80°-deflected *trans*-transoidal form was minimal, the theoretical bands of the  $\pi$ - $\pi^*$  transitions of ( $\varphi_{96} \rightarrow \varphi_{99}$ ) and ( $\varphi_{96} \rightarrow \varphi_{97}$ ) for the phenyl group and the main chain for deflected *trans*-transoidal form were fitted in the observed two-peaks as a function of the deflected angle  $\tau$  using the least square method, and then the other theoretical UV absorption bands were optimized. The helical structure of the chain was not used in the UV calculation because the steric hindrance of the phenyl groups in PPA chain due to the Van der Waals interaction between the side and main chains allowed the  $\pm\tau$ -deflected *trans*-transoidal conformation, but did not allow the considerable helical structures of the chain.<sup>7,9</sup>

Figure 1 shows the back-bone structures of the same deflected *trans* chain conformation projected on a perpendicular plane to its axis. The deflected angle of  $\pm\tau$  corresponds to the  $\pm$ dihedral angle between two double bonds in the main chain. The optimal geometry of various *trans*-transoidal forms against the deflected angle  $\tau$  was calculated in 10° interval from  $\tau=0^\circ$  (*trans*-transoidal) to  $180^\circ$  (*trans*-cisoidal and *cis*-transoidal). The electron charge density of PPA was calculated for optimal conformations in the five-conformer as a function of  $\tau$ .

## RESULTS AND DISCUSSION

Figure 2 shows the UV-Vis spectra of *cis*- and deflected *trans*-PPA in  $\text{CHCl}_3$  in solution, respectively. Solid and dotted lines are the UV-Vis absorption of *cis* and deflected *trans*-PPAs, respectively. In the UV spectrum of *cis*-PPA, there are a broad absorption peak at 263 nm and a plateau peak shoulder at about 390 nm between 300 and 600 nm. On the other hand, there are a sharp absorption peak at 227 nm and a broad peak with the skirts at 248 nm in the UV spectrum of deflected *trans*-PPA.

Here, we will theoretically calculate the UV-Vis absorption bands of five conformers for PPA using CNDO/S.<sup>10</sup> The chain structures of the five conformers in the  $\pi$ - $\pi^*$  transition calculation are the *trans*-transoidal,



**Figure 2.** UV-Vis spectra of (a) *cis*-PPA and (b) deflected *trans*-PPA in  $\text{CHCl}_3$  solution at room temperature.

*trans*-cisoidal, *cis*-transoidal, and  $\pm\tau$ -deflected *trans*-transoidal conformations in an interval of deflected angle  $\tau = 10^\circ$ , as well as those used in previous reports.<sup>7,9</sup>

In the SCF-MO calculation,<sup>12</sup> we used the configuration interaction (CI) method to evaluate the most probable wave function for the true excitation and basis states of  $\pi$ - $\pi^*$  transition, because the respective electron configurations mix in the excitation states, which are restricted between the five highest occupied molecular orbitals and the five lowest unoccupied molecular ones. The molecular orbitals of the five conformers for PPA consisted of 192 basis sets and 192 valence electrons occupying up to the 96-th molecular orbital, and the two-center integrals were estimated based on Nishimoto-Mataga equation.<sup>13</sup>

Figure 3 shows the schematic representation of the orbital energy diagram from  $\varphi_{92}$  to  $\varphi_{101}$  for *cis*-transoidal and 90°-deflected *trans*-transoidal PPAs calculated theoretically. The obtained orbital energies of  $\varphi_{96}$  (HOMO) and  $\varphi_{97}$  (LUMO) are  $E(\varphi_{96}) = -7.664 \text{ kcal mol}^{-1}$  and  $E(\varphi_{97}) = -2.011 \text{ kcal mol}^{-1}$  for *cis*-transoidal PPA, and  $E(\varphi_{96}) = -8.319 \text{ kcal mol}^{-1}$  and  $E(\varphi_{97}) = -1.053 \text{ kcal mol}^{-1}$  for deflected *trans* PPA. Energies for other occupied orbitals from  $\varphi_{91}$  to  $\varphi_{94}$  for deflected *trans*-transoidal PPA are higher than those for *cis*-transoidal PPA and tend to degenerate in energy, while only the energy level of LUMO shows substantial increases in energy among the unoccupied molecular orbitals.

Tables I and II list the calculated transition wavelengths, oscillator strengths, excited molecular orbitals,

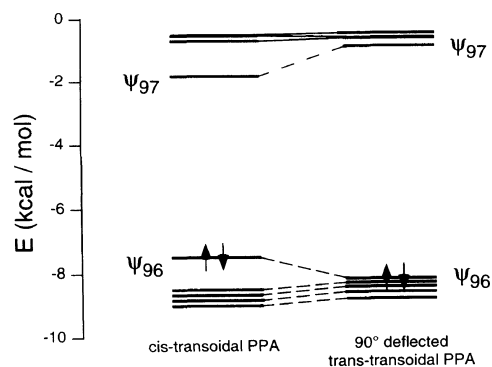


**Figure 3.** Schematic representation of the orbital energy diagram for *cis*-transoidal PPA and 90°-deflected *trans*-transoidal PPA calculated by CNDO/S.

and the CI compositions which represent the relative contribution of the transition. The resultant CI compositions for excited molecular orbitals indicate that the main contribution of 98% at 371.38 nm for *cis*-transoidal PPA, which is attributed to the absorption of the main chain, come from the transition between  $\phi_{96}$  and  $\phi_{97}$ , and the contribution of 84% at 257.93 nm is due to the side chain, mainly the transition between  $\phi_{96}$  and  $\phi_{99}$ . On the other hand, the absorption bands of the main and side chains for the deflected *trans* PPA shift to 275.14 and 248.88 nm with decreases in CI compositions from 98 to 69% and from 84 to 49%, respectively.

Comparisons between the experimental and theoretical UV-Vis spectra of for *cis*-PPA and 90° deflected *trans*-PPA are shown in figure 4. In each figure, discrete solid lines are the theoretical UV absorption on the basis of UV calculation within CNDO/S and the solid line is the experimental absorption data. The theoretical absorption lines of all bands for *cis*- and deflected *trans*-transoidal were optimized.

In Figure 4a, the calculated absorption lines at 257.93 and 371.38 nm for *cis*-transoidal form are due to the  $\pi$ - $\pi^*$  transitions of ( $\phi_{96} \rightarrow \phi_{99}$ ) and ( $\phi_{96} \rightarrow \phi_{97}$ ) for the phenyl group and the conjugated main chain between HOMO and LUMO along their axis direction. They are in good agreement with the wavelengths of 263 and 390 nm in the observed UV-Vis spectrum, respectively, as well as the theoretical wavelengths of further bands. This result indicates that the experimental broad and plateau shoulder peaks are due to the  $\pi$ - $\pi^*$  transition for the phenyl groups and the conjugated main chain, respectively. In Figure 4b, the theoretical UV absorption solid lines of the 90°-deflected *trans*-transoidal chain for PPA localizes in the region between 230 and 300 nm of the experimental spectrum of the solid line. They are in greater agreement with the experimental UV spectra, compared with theoretical result of the 80°-deflected *trans*-transoidal five conformers as shown in Figure 4c. The solid lines at 248.88 and 275.14 nm due to the  $\pi$ - $\pi^*$  absorption bands of the phenyl groups and the conjugated main-chain for the 90° deflected *trans*-transoidal forms agree with the board absorption peaks at 227 and 248 nm in the observed UV spectrum of the solid line. Then, these observed peaks come from the  $\pi$ - $\pi^*$  absorption bands of the phenyl groups and the conjugated main-chain, respectively.

**Table I.** Wavelength, oscillator strength, energy levels of molecular orbitals, and CI composition for *cis*-transoidal PPA calculated by CNDO/S

State	Wave length/ nm	Oscillator strength	MO <sup>a</sup>	CI coeff. <sup>b</sup> / %
1	371.38	1.746	96→97	98
2	317.31	0.001	94→97	55
			95→97	40
3	305.47	0.006	93→97	41
			95→97	37
			94→97	18
4	295.01	0.001	93→97	53
			94→97	24
			95→97	17
5	275.28	0.024	96→98	41
			92→97	21
6	266.30	0.011	96→101	78
			92→101	5
7	257.93	0.004	96→99	84
8	256.81	0.034	92→97	69
			96→98	23
9	240.12	0.007	96→100	83
10	225.56	0.009	94→98	54
			93→98	31

<sup>a</sup> The 96-th and 97-th molecular orbitals corresponded to HOMO and LUMO, respectively. <sup>b</sup> The relative contribution of UV transition.

**Table II.** Wavelength, oscillator strength, energy levels of transition molecular orbitals, and CI composition for 90°-deflected *trans*-transoidal PPA calculated by CNDO/S

State	Wave length/ nm	Oscillator strength	MO <sup>a</sup>	CI coeff. <sup>b</sup> / %
1	292.58	0.063	96→98	58
			96→100	26
2	275.14	0.020	96→97	69
			95→97	18
3	268.87	0.008	95→97	62
			96→97	26
4	259.25	0.142	96→100	28
			96→98	27
			96→99	25
5	255.02	0.021	95→98	73
6	248.88	0.030	96→99	49
			96→100	21
			95→100	15
7	247.27	0.223	94→98	19
			95→99	17
8	237.07	0.009	95→100	36
			94→98	32
9	235.50	0.231	94→97	49
			94→98	35
10	230.02	0.047	94→97	24
			94→99	20
			94→100	18

<sup>a</sup> The 96-th and 97-th molecular orbitals corresponded to HOMO and LUMO, respectively. <sup>b</sup> The relative contribution of UV transition.

Compared with the results of *cis*-PPA, the absorption peaks of the phenyl group and the conjugated main chain in the observed spectrum shift to lower wavelength by 35 nm from 263 to 227 nm and by 142 nm from 390 to 248 nm, respectively, and theoretical ones by 9.05 nm from 257.93 to 248.88 nm and by 96.24 nm from 371.38 to 275.14 nm, respectively. There is in qualitative agreement between theory and experiment on two absorp-

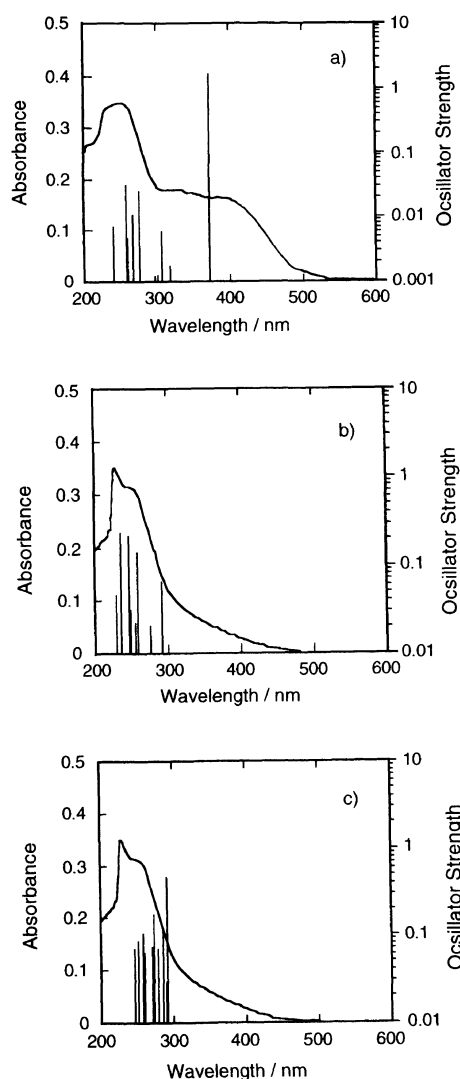


**Figure 4.** The comparison between experimental and theoretical UV-Vis spectra. Discrete solid lines were theoretical UV-Vis absorption bands for *cis*-transoidal PPA (a), 90°-deflected *trans*-transoidal PPA (b), and 80°-deflected *trans*-transoidal PPA calculated using CNDO/S (c).

tion peaks and lower wavelength shift of each peak after thermal isomerization. Thus, the 90°-deflected *trans*-transoidal structure gives the larger energy gap between HOMO-LUMO for phenyl group and main chain, so that the respective  $\pi$ - $\pi^*$  transitions take place in a lower wavelength region, called as blue shift. In Figure 2, the disappearance of the absorption band around 390 nm in the observed UV-Vis spectrum for *trans*-PPA is caused by the blue shift of the conjugated main chain due to 90° deflected *trans*-transoidal structure.

In previous papers,<sup>5-9</sup> we reported from <sup>2</sup>H and <sup>13</sup>C NMR analyses of PPA, based on AM1 molecular orbital method, that after *cis*-*trans* isomerization the 80° deflected *trans*-transoidal conformation of the chain is stable in solid state. Using PM3 approximation in comparison between theory and experiment for the <sup>13</sup>C NMR chemical shifts of the deflected *trans* PPA, the chain conformation was determined to be 75°-deflected *trans*-transoidal form. The determination of the deflected angle depended slightly on the semiempirical molecular orbital methods. As shown in Figure 4a, the observed UV spectrum of solid line does not agree with the

theoretical one for the 80°-deflected *trans*-transoidal conformation in solid state. The deflected angle of the *trans* chain conformation fitted theoretically in Figure 5 increases by 10° in solution. It is considered that the increase of the deflected angle may be due to an oscillational rotation of the chain about the single bond in solution.

On the other hand, we calculated the electron densities of CH and tertiary carbons, referred to as C1 and C2 carbons, respectively, in the conjugated main chain for the five conformers of deflected *trans*-PPA. The electron density of C1 carbon decreased from 4.122 to 4.111 with increasing of the deflected angle and that of the tertiary carbon increased from 4.016 to 4.046. At  $\tau=90^\circ$  the electron densities of C1 and C2 are 4.113 and 4.036, respectively.

These experimental and theoretical facts for PPA indicate that the deflected *trans*-transoidal conformation after thermal isomerization gives rise to the localization of  $\pi$ -electrons in the conjugated main chain, *i.e.*, characteristic blue shift of the  $\pi$ - $\pi^*$  transition absorption in the UV spectrum. We will report theoretically elsewhere in near future how the disagreement of 10° is due to the CNDO/S and AM1 calculation approximations or molecular motions in solution.

## CONCLUSIONS

The UV-Vis spectra of *cis*- and deflected *trans*-transoidal forms for PPA in solution were investigated on the basis of UV-Vis theory within semiempirical molecular orbital method of CNDO/S. The observed UV spectrum for *cis*-PPA consisted of two broadened and shoulder peaks at 263 and about 390 nm, and for deflected *trans*-PPA a sharp peak and broad one with skirts at 227 and 248 nm. The two kinds of UV absorption peaks for each sample were due to the  $\pi$ - $\pi^*$  transitions of the phenyl groups and conjugated main chain. After *cis*-*trans* isomerization, the larger blue shift of the  $\pi$ - $\pi^*$  transition absorption for the conjugated main chain in the UV spectrum came from the localization of  $\pi$ -electrons due to the 90°-deflected structure of the *trans*-transoidal main chain. The increase of the deflected angle from 80° in the solid to 90° in solution may be attributed to an oscillational rotation of the chain about the single bond in solution.

## REFERENCES

1. M. Buchmeiser and R. R. Schrock, *Macromolecules*, **28**, 6642 (1995).
2. A. A. Berlin, M. I. Cherkashin, I. P. Chernysheva, Y. G. Aseyev, Y. I. Barkan, and P. P. Kisilitsa, *Vysokomol. Soyedin*, **9**, 1840 (1967).
3. C. I. Simionescu and V. Percec, *J. Polym. Sci., Polym. Chem. Ed.*, **18**, 147 (1980).
4. A. Furlani, C. Napoletano, M. V. Russo, and W. J. Feast, *Polym. Bull.*, **16**, 311 (1986).
5. T. Kakuchi, S. Matsunami, H. Kamimura, F. Ishii, T. Uesaka, and K. Yokota, *J. Polym. Sci., Part A, Polym. Chem.*, **33**, 1431 (1995).
6. T. Kakuchi, S. Matsunami, H. Kamimura, and F. Ishii, *J. Polym. Sci., Part B, Polym. Phys.*, **33**, 2151 (1995).
7. S. Matsunami, T. Kakuchi, and F. Ishii, *Macromolecules*, **30**, 1074 (1997).

8. T. Kakuchi, S. Matsunami, K. Tsuda, and F. Ishii, *Polym. Bull.*, **40**, 533 (1998).
9. F. Ishii, T. Kakuchi, and S. Matsunami, submitted to *J. Polym. Sci., Part B, Polym. Phys.*
10. J. D. Bene and H. H. Jaffe, *J. Chem. Phys.*, **48**, 4050 (1968).
11. S. Matsunami, T. Watanabe, H. Kamimura, T. Kakuchi, F. Ishii, and K. Tsuda, *Polymer*, **37**, 4853 (1996).
12. J. A. Pople and G. A. Segal, *J. Chem. Phys.*, **44**, 3289 (1966).
13. K. Nishimoto and N. Mataga, *Z. Physik. Chem.*, **12**, 335 (1957).